Inhibition of splitting of confining and chiral transition by rotation.

Pracheta Singha

Victor E. Ambrus, Maxim N. Chernodub.

2407.07828 [hep-ph]

The 8th International Conference on Chirality, Vorticity and Magnetic Field in Quantum Matter.

Table of Contents

1. Motivation
2. formalism
3. Results and Discussion

Motivation

- Properties of Quark-Gluon-Plasma (QGP):
  - Underlying symmetries.
  - equation of state and medium thermodynamics.
  - Phase structure.

In the presence of :

  - finite temperature (T).
  - finite chemical potential (μ).
  - finite rotation (Ω).

Motivation

- Properties of Quark-Gluon-Plasma (QGP):
  - Underlying symmetries.
  - equation of state and medium thermodynamics.
  - Phase structure.

In the presence of :

- finite temperature (T).
- finite chemical potential (μ).
- finite rotation (Ω).

Motivation

- Angular momentum in noncentral collisions $\approx 1000\hbar \implies$ A strong vortical structure of the resulting fluid.

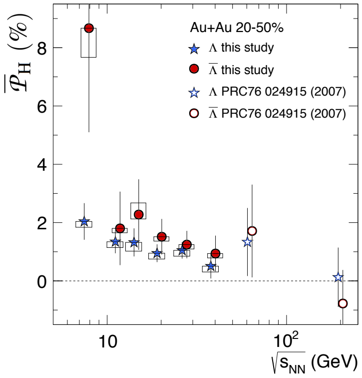

Figure 1: The hyperon average polarization in Au-Au collision . STAR collaboration. Nature 548, 62–65 (2017)

- $\bar{\mathcal{P}}_{\rm H} \equiv \langle \mathcal{P}_H \cdot \hat{J}_{\rm sys} \rangle$
- $\hat{J}_{\rm sys} \equiv$ Direction of the angular momentum of the collision.
- $\mathcal{P}_{\rm H} \equiv$ Hyperon polarization vector in the hyperon rest frame.
- The Fluid vorticity can be estimated from the data $\implies$ "most vortical fluid produced in the laboratory" .

STAR collaboration. Nature 548, 62–65 (2017)

Becattini et al, Phys. Rev. C 95, 054902, (2017)

STAR collaboration. Phys.Rev.C76:024915 (2007)

Motivation

- Presence of vorticity in the system will affect the thermodynamic properties and the phase structure of the QGP.
- Lattice result : Increasing angular velocity increases the transition temperature. Braguta et al. Phys. Rev. D 103, 094515 (2021) , Ji-Chong Yang et al arXiv:2307.05755 [hep-lat]
- Effective model studies: without boundary condition:

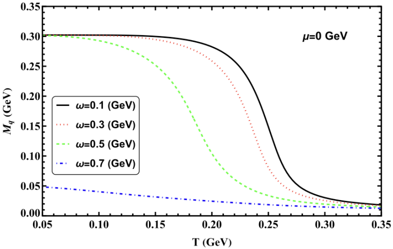

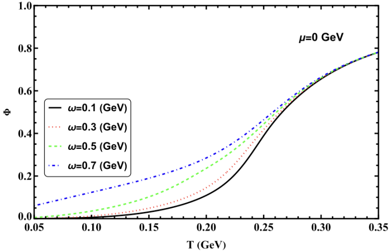

Figure 2: Temperature variation of effective quark mass and traced Polyakov loop. Mei Huang et al, PhysRevD.108.096007, (2023)

Motivation

- Presence of vorticity in the system will affect the thermodynamic properties and the phase structure of the QGP.
- Lattice result : Increasing angular velocity increases the transition temperature. Braguta et al. Phys. Rev. D 103, 094515 (2021) , Ji-Chong Yang et al arXiv:2307.05755 [hep-lat]
- Effective model studies: with boundary condition:

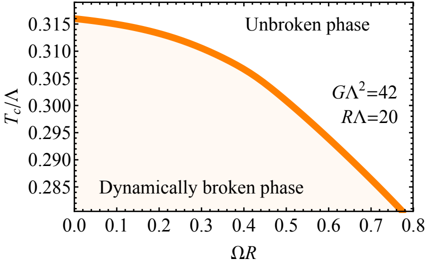

Figure 2: Chiral phase diagram in $T - \Omega R$ plane with MIT boundary condition . M.N. Chernodub et al. JHEP 01 (2017) 136

- The qualitative behaviour of the chiral phase diagram remains the same with or without boundary condition.

Motivation

- Effective model studies: with boundary condition:

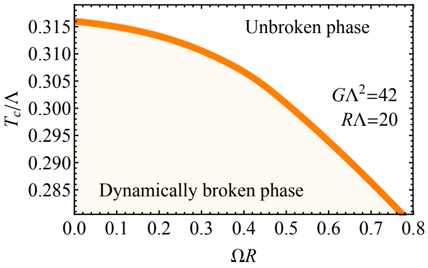

Figure 2: Chiral phase diagram in $T - \Omega R$ plane with MIT boundary condition . M.N. Chernodub et al. JHEP 01 (2017) 136

- The qualitative behaviour of the chiral phase diagram remains the same with or without boundary condition.

- Objective 1 :

The Deconfinement phase transtion in a rotating Bounded system.

Motivation

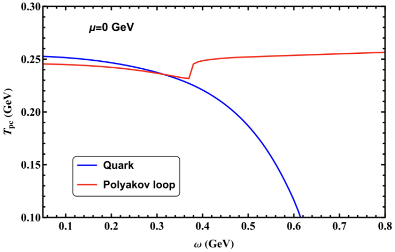

Figure 3: Chiral and deconfinement phase digram in $T - \Omega$ plane . Mei Huang et al, PhysRevD.108.096007, (2023)

- A rotation induced split between chiral and deconfinement phase transition was reported in Mei Huang et al, PhysRevD.108.096007, (2023)

- Objective 2 :

Is there a split between chiral and Deconfinement phase diagram for a rotating bounded system?

Polyakov Linear Sigma model with Quarks

- Model Lagrangian:

$$\mathcal{L}(\phi, \psi, L) = \mathcal{L}_{\mathcal{M}}(\phi) + \mathcal{L}_q(\phi, \psi, L) + \mathcal{L}_L(L)\,.$$

- Mesonic contribution:

$$\mathcal{L}_{\mathcal{M}}(\phi) = \frac{1}{2}\left(\partial_\mu \sigma \partial^\mu \sigma + \partial_\mu \vec{\pi} \partial^\mu \vec{\pi}\right) - V_{\mathcal{M}}(\sigma, \vec{\pi})\,,$$

$$V_{\mathcal{M}}(\sigma, \vec{\pi}) = \frac{\lambda}{4}\left(\sigma^2 + \vec{\pi}^2 - v^2\right)^2 - h\sigma\,.$$

- Quark contribution:

$$\mathcal{L}_q = \bar{\psi}\left(i\not{D} - g\phi\right)\psi \equiv \bar{\psi}\left[i\not{D} - g(\sigma + i\gamma_5 \vec{\tau}\cdot\vec{\pi})\right]\psi$$

Polyakov Linear Sigma model with Quarks

- Mesonic contribution:

$$\mathcal{L}_{\mathcal{M}}(\phi) = \frac{1}{2}\left(\partial_\mu\sigma\partial^\mu\sigma + \partial_\mu\vec{\pi}\partial^\mu\vec{\pi}\right) - V_{\mathcal{M}}(\sigma,\vec{\pi}),$$
$$V_{\mathcal{M}}(\sigma,\vec{\pi}) = \frac{\lambda}{4}\left(\sigma^2 + \vec{\pi}^2 - v^2\right)^2 - h\sigma .$$

- Quark contribution:

$$\mathcal{L}_q = \bar{\psi}\left(i\not{D} - g\phi\right)\psi \equiv \bar{\psi}(i\not{D})\psi - g\bar{\psi}(\sigma + i\gamma_5\vec{\tau}\cdot\vec{\pi})\psi$$

- $h\sigma \equiv$ explicit chiral symmetry breaking $\to m_\pi \neq 0$.
- Model parameters: $\lambda,\ v,\ g,\ h$, are fixed by $m_\pi,\ f_\pi,\ m_\sigma,\ m_q$.

Polyakov Linear Sigma model with Quarks

- Model Lagrangian:

$$\mathcal{L}(\phi, \psi, L) = \mathcal{L}_{\mathcal{M}}(\phi) + \mathcal{L}_q(\phi, \psi, L) + \mathcal{L}_L(L) \,.$$

- Polyakov contribution:

$$\frac{\mathcal{L}_L}{T^4} = \frac{a(T) L^* L}{2} - b(T) \ln \left[1 - 6 L^* L + 4 \left(L^{*3} + L^3 \right) - 3 (L^* L)^2 \right]$$

Polyakov Linear Sigma model with Quarks

- Polyakov contribution:

$$\frac{\mathcal{L}_L}{T^4} = \frac{a(T)L^* L}{2} - b(T) \ln \left[1 - 6L^* L + 4\left(L^{*3} + L^3\right) - 3(L^* L)^2\right]$$

- Quark contribution:

$$\mathcal{L}_q = \bar{\psi}\left(i\not{D} - g\phi\right)\psi \equiv \bar{\psi}\left[i\not{D} - g(\sigma + i\gamma_5 \vec{\tau}\cdot\vec{\pi})\right]\psi$$

$$D^\mu = \partial^\mu - iA^\mu \qquad A^\mu = \delta_{\mu 0} A^0$$

Polyakov Linear Sigma model with Quarks

- Polyakov contribution:

$$\frac{\mathcal{L}_L}{T^4} = \frac{a(T)L^*L}{2} - b(T)\ln\left[1 - 6L^*L + 4\left(L^{*3} + L^3\right) - 3(L^*L)^2\right]$$

- Quark contribution:

$$\mathcal{L}_q = \bar{\psi}\left(i\not{D} - g\phi\right)\psi \equiv \bar{\psi}\left[i\not{D} - g(\sigma + i\gamma_5\vec{\tau}\cdot\vec{\pi})\right]\psi$$

$$D^\mu = \partial^\mu - iA^\mu \qquad A^\mu = \delta_{\mu 0}A^0$$

$$L = \frac{1}{3}\mathrm{Tr}\left(\mathcal{T}\exp[i\int_0^\beta d\tau \mathcal{A}_4(\vec{x},\tau)]\right)$$

Polyakov Linear Sigma model with Quarks

- Polyakov contribution:

$$\frac{\mathcal{L}_L}{T^4} = \frac{a(T)L^*L}{2} - b(T)\ln\left[1 - 6L^*L + 4\left(L^{*3} + L^3\right) - 3(L^*L)^2\right]$$

- L and L^* are the order parameter for the confinement deconfinement phase transition as $\langle L\rangle = e^{-\beta F_q},\ m_q \to \infty$.
- $a(T)$ and $b(T)$ are fitted to reproduce Lattice SU(3) pure gauge results.

Thermodynamic potential

- Thermodynamic potential:

$$Z = \mathrm{Tr}\left(\mathrm{e}^{-\beta(H-\mu N)}\right)$$

$$F(T) = -\frac{T\ln\mathcal{Z}}{V} = V_{\mathcal{M}} + V_L + F_{\psi\bar{\psi}}$$

where,

$$F_{\psi\bar{\psi}} = -2N_f T \sum_{\varsigma=\pm 1} \int \frac{d^3p}{(2\pi)^3} F_{\varsigma}\,.$$

$$F_+ = \ln\left[1 + 3Le^{-\beta\mathcal{E}_+} + 3L^* e^{-2\beta\mathcal{E}_+} + e^{-3\beta\mathcal{E}_+}\right],$$

$$F_- = \ln\left[1 + 3L^* e^{-\beta\mathcal{E}_-} + 3Le^{-2\beta\mathcal{E}_-} + e^{-3\beta\mathcal{E}_-}\right].$$

Thermodynamic potential

- Thermodynamic potential:

$$Z = \mathrm{Tr}\left(\mathrm{e}^{-\beta(H-\mu N)}\right)$$

$$F(T) = -\frac{T\ln\mathcal{Z}}{V} = V_{\mathcal{M}} + V_L + F_{\psi\bar{\psi}}$$

- Saddle point equations:

$$\frac{\partial(F_{\psi\bar{\psi}} + V_{\mathcal{M}})}{\partial\sigma} = 0\,; \quad \frac{\partial(F_{\psi\bar{\psi}} + V_L)}{\partial L} = 0\,; \quad \frac{\partial(F_{\psi\bar{\psi}} + V_L)}{\partial L^*} = 0$$

- All thermodynamic observables are evaluated from the thermodynamic potential $F(\sigma_{\mathrm{mf}}, L_{\mathrm{mf}}, L^*_{\mathrm{mf}})$

Phase transition

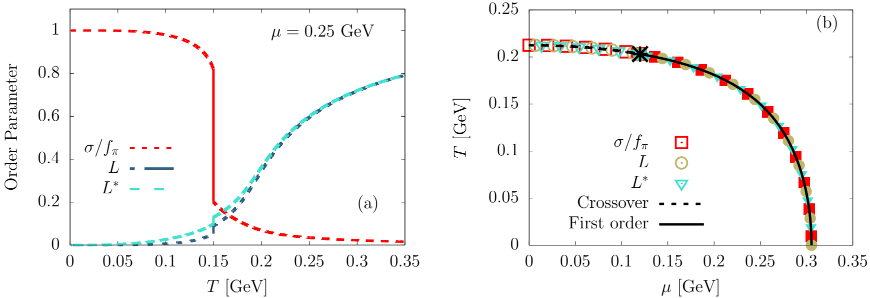

Figure 4: Phase transition at nonzero temperature and chemical potential (left) and corresponding phase diagram (right)

- Increasing $\mu \implies$ crossover $\rightarrow$ first order phase transtion.
- $(T_c, \mu_c) = (0.2043, 0.1123)$ in GeV.

Rotating cylindrical system

- Cylinder of radius R rigidly rotating about the z axis in the counterclockwise direction.
- We assume the effects of rotation on to the quark sector.
- Conservation of angular momentum J_z.
- Causality criteria : $\Omega R \leq 1$.
- Transverse direction is finite $\Longrightarrow$ transverse momentum is discrete.

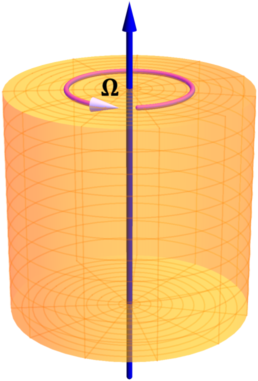

Figure 5: Rigidly rotating cylinder M.N. Chernodub et. al. 10.1007/JHEP01(2017)136.

Rotating cylindrical system

- The quark Lagrangian:

$$\mathcal{L}_{\mathrm{E}} = \bar{\psi}\left[\gamma^0\left(-\partial_\tau + \Omega J^z + i\mathcal{A}_4 + \mu\right) + i\gamma \cdot \nabla - g\sigma\right]\psi\,.$$

- Frequency : $\tilde{\omega}^a = \omega^a - \Omega m$
  where ω^a is the Minkowski frequency, with contribution from the energy, chemical potential and background gauge field.
- Energy: $E = \sqrt{p^2 + g^2\sigma^2}$; with $p = \sqrt{q^2 + p_z^2}$
- Spectral boundary condition :

$$qR = \begin{cases} \xi_{m-\frac{1}{2},\ell}, & m > 0\,, \\ \xi_{-m-\frac{1}{2},\ell}, & m < 0\,. \end{cases}$$

Here ξ_{nl} is the l_{th} nonzero root of the Bessel function.

Modified free energy including rotation

- Quark contribution to the free energy:

$$F_{\psi\bar{\psi}} = -\frac{2N_f T}{\pi R^2} \sum_{l=1}^{\infty} \sum_{m=-\infty}^{\infty} \int \frac{dp_z}{2\pi} \tilde{F}_{\varsigma} \,.$$

$$\tilde{F}_{+} = \ln\left[1 + 3Le^{-\beta\tilde{\mathcal{E}}_{+}} + 3L^{*}e^{-2\beta\tilde{\mathcal{E}}_{+}} + e^{-3\beta\tilde{\mathcal{E}}_{+}}\right],$$

$$\tilde{F}_{-} = \ln\left[1 + 3L^{*}e^{-\beta\tilde{\mathcal{E}}_{-}} + 3Le^{-2\beta\tilde{\mathcal{E}}_{-}} + e^{-3\beta\tilde{\mathcal{E}}_{-}}\right].$$

- Non rotating system $\rightarrow$ rotating bounded system:

$$Z \rightarrow \mathrm{Tr}\left(\mathrm{e}^{-\beta(H-\mu N-\Omega J_z)}\right); \quad \int \frac{d^3p}{(2\pi)^3} \rightarrow \frac{1}{\pi R^2} \sum_{l=1}^{\infty} \sum_{m=-\infty}^{\infty} \int \frac{dp_z}{2\pi}$$

$$\mathcal{E}_{\pm} = \left(p^2 + g^2\sigma^2\right)^{\frac{1}{2}} \mp \mu \rightarrow \tilde{\mathcal{E}}_{\pm} = \left(p_z^2 + \frac{\xi_{nl}^2}{R^2} + g^2\sigma^2\right)^{\frac{1}{2}} - \Omega m \mp \mu$$

Phase transition in bounded system

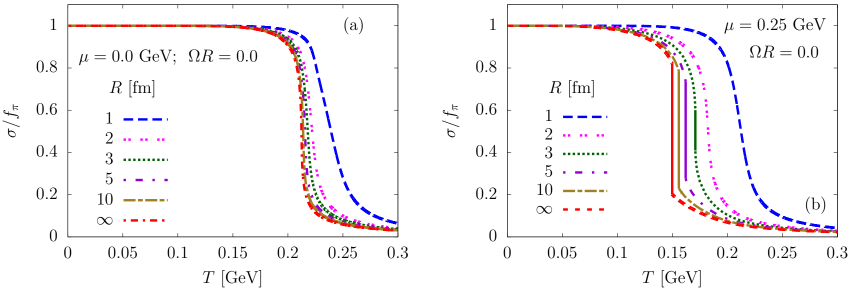

Figure 6: Temperature variation of sigma for different Radii at zero (left) and nonzero (right) chemical potential

- Boundary favours the corossover transtion over the first order.

Phase transition in bounded system

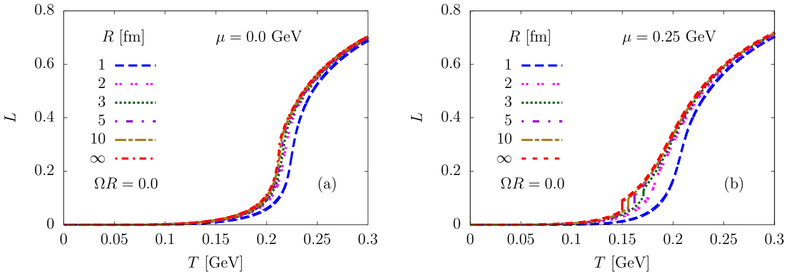

Figure 7: Temperature variation of traced Polyakov loop for different Radii at zero (left) and nonzero (right) chemical potential

- First order signature is much suppressed in Polyakov loop behavior.

Phase Diagram in bounded system

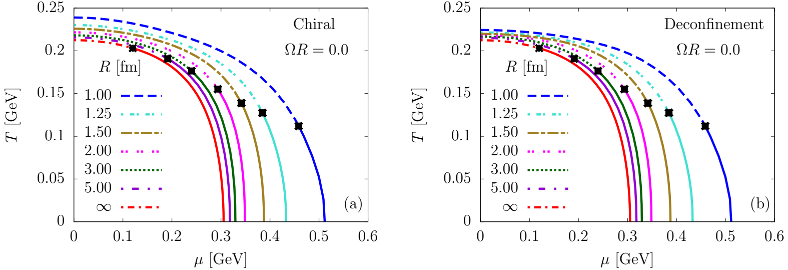

Figure 8: The phase diagram of bounded system for chiral (a) and Deconfinement (b) transition for different R .

- Boundary effects drags the critical point towards increasing μ for both chiral and deconfinement phase transition .

Splitting in bounded system

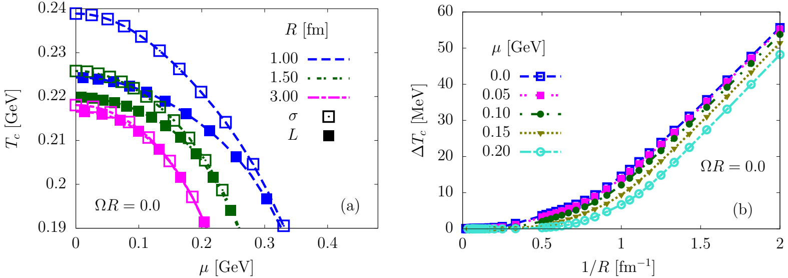

Figure 9: T_c as a function of μ for chiral and deconfinement transition (a) and the split in T_c as a function of the inverse radius.(b)

- Boundary effects introduces a splitting[2] between the chiral and confinement-deconfinement crossover. $\Delta T_c = T_c^{(\sigma)} - T_c^{(L)}$.
- As R decreases splitting increases.

[2] Mei Huang et al. Phys.Rev.D 108 (2023) 9, 096007

Phase transition at finite rotation

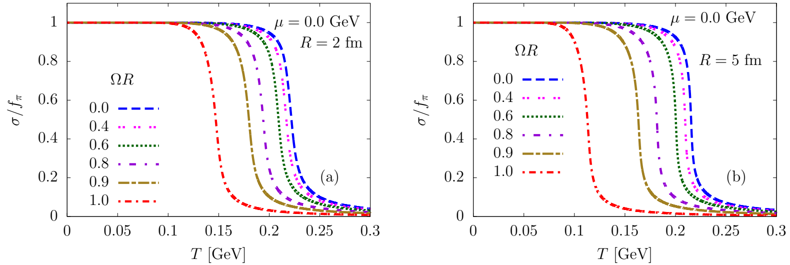

Figure 10: σ/f_π as a function of temperature for Radii 2 fm (a) and 5 fm (b) for $\mu = 0$.

- Critical temperature decreases as angular velocity increase.

Phase transition at finite rotation

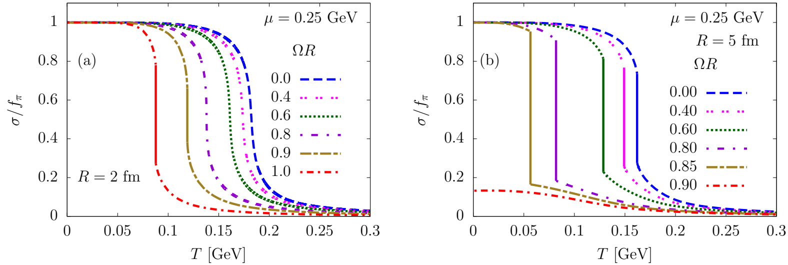

Figure 11: σ/f_π as a function of temperature for Radii 2 fm (a) and 5 fm (b) for $\mu = 0.25$ GeV .

- For finite temperature and chemical potential , angular velocity can induce first order phase transition.

Phase diagram : R 2 fm

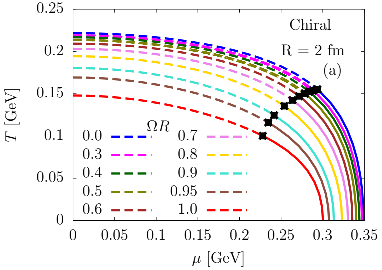

Figure 12: Phase diagram with different angular velocities for chiral (a) and Deconfinement (b) phase transition.

- Finite rotation drags down the critical point towards lower chemical potential.

Phase diagram : R 5 fm

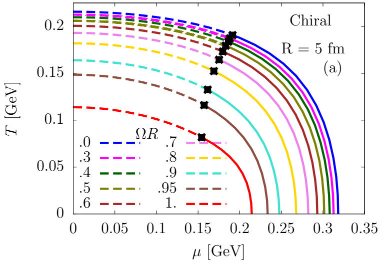

Figure 13: Phase diagram with different angular velocities for chiral (a) and Deconfinement (b) phase transition.

- Finite rotation drags down the critical point towards lower chemical potential.

Splitting at nonzero rotation

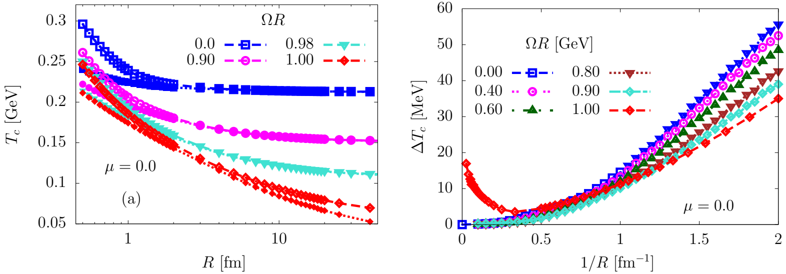

Figure 14: (a) T_c as a function of R for chiral and deconfinement transtion and (b) their difference as a function of 1/R at different values of ΩR.

- At zero chemical potential as R decreases splitting increases.
- Non-triviality in the splitting of transition points as $\Omega R \to 1$.

Splitting at nonzero rotation

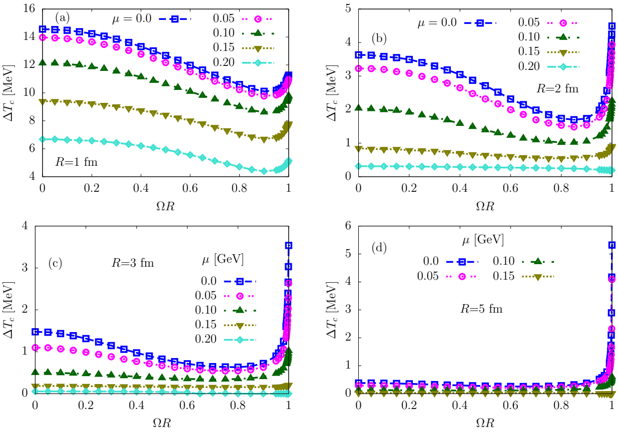

Figure 15: ΔT_c as a function of ΩR for different μ and different radii.

- The split decreases as ΩR increases .

Discussion

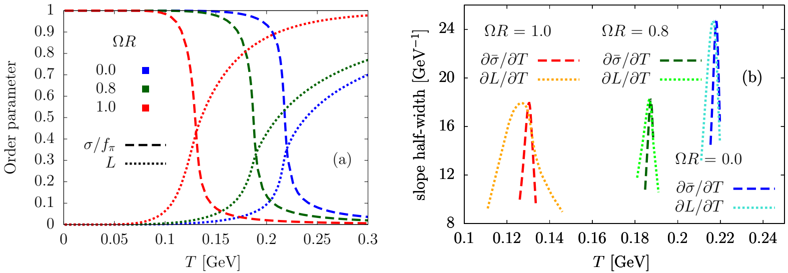

Figure 16: Order parameters and their slopes as a function of T at R=3 fm $\mu = 0$ and 3 values of angular velocity.

- A discussion of a unique value for T_c and hence the identification of a split is not unambiguous in the case of rotating systems.

Discussion

- Polyakov enhanced Linear Sigma model coupled to the quark degrees of freedom is employed to study QCD phase structure and $T \neq 0; \mu \neq 0$ results are reproduced.
- Boundary effects favour the crossover scenario and drags the critical endpoint towards higher chemical potential.
- Boundary effects mediates a splitting between chiral and confinement deconfinement crossovers .
- splitting decreases as R increases.
- For a fixed R as ΩR increases splitting decreases.
- With Increasing rotation the phase transition temperature and critical chemical potential decreases.

Acknowlegement: This work is supported by the European Union - NextGenerationEU through grant No. 760079/23.05.2023, funded by the Romanian ministry of re- search, innovation and digitalization through Romania's National Recovery and Resilience Plan, call no. PNRR-III-C9-2022-I8.

Thank You For Your Attention!!

Self-adjointness of the Hamiltonian

- On a general space-time, the Dirac inner product can be written as:

$$\psi, \chi = \int_V d^3x \sqrt{-g}\ \gamma^t \chi,$$

  where V is the volume enclosed inside the boundary and $\{\gamma^\mu, \gamma^\nu\} = -2g^{\mu\nu}$.
- The Hamiltonian is self-adjoint if:

$$\psi, H\chi = H\psi, \chi.$$

- Writing the Dirac equation as $H\psi = i\partial_t\psi$ gives:

$$\psi, H\chi - H\psi, \chi = -\, i \int_{\partial V} d\Sigma_i \sqrt{-g}\ e^i_{\gamma^\chi=0},$$

  where ∂V is the boundary of V.
- For a cylindrical boundary at $\rho = R \leq \Omega^{-1}$:

$$R \int_{-\infty}^{\infty} dz \int_0^{2\pi} d\varphi\, \gamma^{\hat{\rho}} \chi = 0.$$

Spectral boundary conditions[3]

- Consider the Fourier transform of a solution ψ of the Dirac equation:

$$\psi = \sum_{m=-\infty}^{\infty} e^{i(m+\frac{1}{2})\varphi}(e^{-\frac{i}{2}\varphi}\psi^1_{m+\frac{1}{2}}, e^{\frac{i}{2}\varphi}\psi^2_{m+\frac{1}{2}}, e^{-\frac{i}{2}\varphi}\psi^3_{m+\frac{1}{2}}, e^{\frac{i}{2}\varphi}\psi^4_{m+\frac{1}{2}})^T.$$

- Its charge conjugate $\psi_c = i\gamma^2\psi^*$ is given by:

$$\psi_c = \sum_{m=-\infty}^{\infty} e^{i(m+\frac{1}{2})\varphi}(e^{-\frac{i}{2}\varphi}\psi^{4\,*}_{-m-\frac{1}{2}}, -e^{\frac{i}{2}\varphi}\psi^{3\,*}_{-m-\frac{1}{2}}, -e^{-\frac{i}{2}\varphi}\psi^{2\,*}_{-m-\frac{1}{2}}, e^{\frac{i}{2}\varphi}\psi^{1\,*}_{-m-\frac{1}{2}})^T.$$

- The self-adjointness of the Hamiltonian is then ensured if:

$$(\psi,\chi): \quad \sum_{m=-\infty}^{\infty}\left(\psi^{1\,*}_{m+\frac{1}{2}}\chi^4_{m+\frac{1}{2}} + \psi^{2\,*}_{m+\frac{1}{2}}\chi^3_{m+\frac{1}{2}} + \psi^{3\,*}_{m+\frac{1}{2}}\chi^2_{m+\frac{1}{2}} + \psi^{4\,*}_{m+\frac{1}{2}}\chi^1_{m+\frac{1}{2}}\right) = 0,$$

$$(\psi_c,\chi): \sum_{m=-\infty}^{\infty}\left(\psi^1_{m+\frac{1}{2}}\chi^1_{-m-\frac{1}{2}} - \psi^2_{m+\frac{1}{2}}\chi^2_{-m-\frac{1}{2}} - \psi^3_{m+\frac{1}{2}}\chi^3_{-m-\frac{1}{2}} + \psi^4_{m+\frac{1}{2}}\chi^4_{-m-\frac{1}{2}}\right) = 0.$$

- Solution:

$$m+\tfrac{1}{2} > 0 \;: J_m(q_m R) = 0 \quad \text{such that } \psi^1_{m+\frac{1}{2}}\rfloor_{\rho=R} = \psi^3_{m+\frac{1}{2}}\rfloor_{\rho=R} = 0;$$

$$m+\tfrac{1}{2} < 0 \;: J_{m+1}(q_m R) = 0 \text{ such that } \psi^2_{m+\frac{1}{2}}\rfloor_{\rho=R} = \psi^4_{m+\frac{1}{2}}\rfloor_{\rho=R} = 0.$$

[3] M. Hortaçsu, K. D. Rothe, B. Schroer, Nucl. Phys. B **171**, 530 (1980).